NATIONAL ADVISORY COMMITTEE FOR AERONAUTICS

TECHNICAL NOTE 2316

WIND-TUNNEL INVESTIGATION AT LOW SPEED OF LATERAL CONTROL CHARACTERISTICS OF AN UNTAPERED 45° SWEPTBACK SEMISPAN WING OF ASPECT RATIO 1.59 EQUIPPED WITH VARIOUS 25-PERCENT-CHORD PLAIN AILERONS

By Harold S. Johnson and John R. Hagerman

Langley Aeronautical Laboratory
Langley Field, Va.

Washington
March 1951

NATIONAL ADVISORY COMMITTEE FOR AERONAUTICS

TECHNICAL NOTE 2316

WIND-TUNNEL INVESTIGATION AT LOW SPEED OF LATERAL CONTROL CHARACTERISTICS OF AN UNTAPERED 45° SWEPTBACK SEMISPAN WING OF ASPECT RATIO 1.59 EQUIPPED WITH VARIOUS 25-PERCENT-CHORD PLAIN AILERONS

By Harold S. Johnson and John R. Hagerman

SUMMARY

A wind-tunnel investigation was made at low speed to determine the lateral control characteristics of a 45° sweptback untapered semispan wing of aspect ratio 1.59 equipped with 25-percent-chord plain unsealed ailerons having various spans and spanwise locations.

The results of the investigation indicated that the aileron effectiveness increased as the aileron span was increased and that a partial-span aileron was most effective in producing rolling moment when located outboard on the wing semispan. The change of hinge-moment coefficient with angle of attack and aileron deflections at low angles were only slightly affected by aileron span. Existing empirical relationships for predicting the aileron effectiveness parameter C_{l_δ} and the aileron hinge-moment parameter C_{h_δ} gave satisfactory agreement with the experimental results. The aileron hinge-moment parameter C_{h_α} could not be predicted satisfactorily for all spans of ailerons.

INTRODUCTION

The National Advisory Committee for Aeronautics is making an extensive investigation of the lift and control effectiveness of various flaps and control surfaces on wings having plan forms suitable for transonic and supersonic airplanes. The objective is to obtain flap- and aileron-design criterions similar to those available for wings of conventional low-speed plan forms (references 1 to 3). As

part of this broad study, the lift and lateral control characteristics of an untapered low-aspect-ratio semispan wing having various amounts of sweep and equipped with 25-percent-chord plain unsealed flaps or ailerons of various spans and spanwise locations are being investigated in the Langley 300 MPH 7- by 10-foot tunnel.

This paper presents the results of the investigation of a 45° sweptback wing configuration having an aspect ratio of 1.59 and utilizing the 25-percent-chord control surfaces as ailerons. Rolling-moment, yawing-moment, and aileron hinge-moment data were obtained through an aileron-deflection range from -30° to 30° at constant angles of attack ranging from -4 to about the angle of maximum lift.

The results of an investigation of the same semispan wing utilizing the 25-percent-chord control surfaces as lift flaps are presented in reference 4. Investigations of the model at 0° of sweep and aspect ratio 3.13 with the control surfaces used as flaps and ailerons are reported in references 5 and 6, respectively.

SYMBOLS

The forces and moments measured on the wing are presented about the wind axes which, for the conditions of these tests (zero yaw), correspond to the stability axes. The pitching-moment, rolling-moment, and yawing-moment data are presented about the axes through the origin located at the 25-percent-chord station of the mean aerodynamic chord (fig. 1).

The rolling-moment-coefficient and yawing-moment-coefficient data presented herein represent the aerodynamic effects on a complete wing produced by the deflection of the aileron on only the right semispan of the complete wing.

C_L	lift coefficient (Twice lift of semispan model/qS)
C_D	drag coefficient (Twice drag of semispan model/qS)
C_m	pitching-moment coefficient (Twice pitching moment of semispan model/$qS\bar{c}$)
C_l	rolling-moment coefficient (L/qSb)
C_n	yawing-moment coefficient (N/qSb)

C_h	aileron hinge-moment coefficient $\left(H/2qM_1\right)$
L	rolling moment resulting from aileron deflection, foot-pounds
N	yawing moment resulting from aileron deflection, foot-pounds
H	aileron hinge moment, foot-pounds
M_1	area moment of aileron rearward of and about hinge axis, feet^3 (see table I)
q	free-stream dynamic pressure, pounds per square foot $\left(\frac{1}{2}\rho V^2\right)$
S	twice area of semispan wing model, 19.32 square feet
b	twice span of semispan model, 5.55 feet
$\bar{c}$	wing mean aerodynamic chord, 3.52 feet
c	local wing chord, feet
y	lateral distance from plane of symmetry, measured perpendicular to plane of symmetry, feet
b_a	span of aileron, measured perpendicular to plane of symmetry, feet
V	free-stream velocity, feet per second
ρ	mass density of air, slugs per cubic foot
α	angle of attack of wing chord measured at plane of symmetry, degrees
δ_a	aileron deflection relative to wing chord plane, measured perpendicular to aileron hinge axis (positive when trailing edge is down), degrees
α_δ	control effectiveness parameter; that is, effective change in angle of attack caused by unit angular change in control-surface deflection

$$C_{l_\delta} = \left(\frac{\partial C_l}{\partial \delta_a}\right)_\alpha$$

$$C_{h_\alpha} = \left(\frac{\partial C_h}{\partial \alpha}\right)_{\delta_a}$$

$$C_{h_\delta} = \left(\frac{\partial C_h}{\partial \delta_a}\right)_{\alpha}$$

The subscripts outside the parentheses indicate the factor held constant. The parameters were measured at an angle of attack or an aileron deflection of 0°.

Subscripts:

a_i inboard end of aileron at hinge line

a_o outboard end of aileron at hinge line

CORRECTIONS

Jet-boundary corrections, determined by the method presented in reference 7, have been applied to the angle-of-attack and drag-coefficient values. Blockage corrections, to account for the constriction effects of the model and its wake, have also been applied to the test data (reference 8). The rolling-moment data were corrected for reflection-plane effects by the method of reference 9 by using unpublished experimental data for low-aspect-ratio wings. (See fig. 2). No corrections have been applied to the data to account for the very small amount of wing twist produced by aileron deflection or for the small effect of air-flow leakage around the end plate at the root of the model.

MODEL AND APPARATUS

The semispan-wing model used in the investigation was constructed of laminated mahogany over a solid steel spar. The plan-form dimensions are shown in figure 1. The wing sections normal to the leading edge were NACA 64A010 and the model had an aspect ratio of 1.59 (based on full-span dimensions), a taper ratio of 1.0, and 45° of sweepback. The wing model had neither twist nor dihedral. This model was also used for the investigations reported in references 4 to 6.

Details of the 25-percent-chord plain unsealed ailerons are shown in figure 1. The ailerons were constructed of mahogany with steel spars and had joints at three spanwise stations so that various spans of ailerons at various spanwise locations could be investigated (fig. 1 and table I). When two or more aileron segments were tested in combination, the chordwise gaps between the aileron segments were sealed. A motor-driven aileron-actuating mechanism was used to obtain the various aileron deflections which were constantly indicated by the use of a calibrated potentiometer. The aileron hinge moments were measured by means of a calibrated electrical resistance type of strain gage.

The semispan wing model was mounted vertically in the Langley 300 MPH 7- by 10-foot tunnel, which is a closed-throat single-return tunnel. The root chord of the model was adjacent to the ceiling of the tunnel, which served as a reflection plane (fig. 3). The model was mounted on the six-component balance system so that all forces and moments acting on the model could be measured. A small clearance was maintained between the model and the tunnel ceiling so that no part of the model came into contact with the tunnel structure. A $\frac{1}{16}$-inch-thick metal end plate was attached to the root of the model (fig. 3) to deflect the air flowing into the test section through the clearance hole in order to minimize the effect of this spanwise air flow on the flow over the model.

TESTS

All the tests were made at an average dynamic pressure of approximately 100 pounds per square foot, which corresponds to a Mach number of 0.27 and a Reynolds number of about 6.3×10^6 based on the wing mean aerodynamic chord of 3.52 feet. Measurements have indicated that the tunnel turbulence factor is very close to unity.

The lateral-control tests with the various span ailerons were made through an aileron-deflection range from -30° to 30° at constant angles of attack ranging from -4° to about 24° in approximately 4° increments.

RESULTS AND DISCUSSION

Wing Aerodynamic Characteristics

The lift, drag, and pitching-moment characteristics of the plain wing model are presented in figure 4. Because these data have been previously discussed in reference 4, where additional data for the wing with the various-span control surfaces used as lift flaps have been presented, no discussion is presented herein.

Aileron Control Characteristics

The variation of the aileron lateral control characteristics with aileron deflection is presented in figures 5 to 8 for the four spans of outboard ailerons $\left(y_{a_o} = 0.955\frac{b}{2}\right)$ and in figures 9 and 10 for the approximately half-span ailerons at the inboard and midsemispan locations, respectively. A comparison of the experimental and estimated lateral-control parameters C_{h_α}, C_{h_δ}, and C_{l_δ} for the model equipped with outboard ailerons is presented in figure 11.

Rolling-moment characteristics.- At angles of attack of less than about 12.4°, the rolling-moment coefficients for the wing equipped with outboard ailerons varied nearly linearly with aileron deflection and were relatively unaffected by angle-of-attack variations (figs. 5 to 8). At a given aileron deflection, as the angle of attack was increased above $\alpha = 12.4^{\circ}$, the rolling-moment coefficients generally decreased and this decrease was largest at high aileron deflections. As expected, the rolling-moment coefficient at a given aileron deflection increased as the span of the outboard aileron was increased (figs. 5 to 8) although only a slight increase resulted from increasing the span from $0.637\frac{b}{2}$ to $0.875\frac{b}{2}$ (figs. 7 and 8). A study of the data for the approximately half-span ailerons at the three spanwise locations investigated (figs. 6, 9, and 10) reveals that except for some high angles of attack the rolling-moment coefficient increased as the aileron was moved outboard. The variation of C_l with α is smallest in relative magnitude for the half-span aileron at the midsemispan location and greatest for the aileron located at the wing tip. This greater decrease in C_l with increasing α for the outboard aileron is believed to result from the spanwise air flow in the tip region of a sweptback wing at high angles of attack. The variation of C_l with aileron deflection is similar to, but of considerably smaller magnitude than, that exhibited by

the wing at 0° of sweepback and aspect ratio of 3.13 as reported in reference 6. The effects of angle-of-attack variations are greater for the 45° sweptback configuration, especially for the outboard ailerons, probably because of the spanwise air flow in the tip region. This comparison shows that the effects of increasing the angle of sweepback and decreasing the aspect ratio on the aileron effectiveness were as expected.

As would be expected (references 3 and 10) and as indicated previously, the experimental data for the model equipped with outboard ailerons (fig. 11 and table I) show that the aileron effectiveness parameter C_{l_δ} increased with increasing aileron span and that this variation of C_{l_δ} with aileron span was nonlinear. Estimated values of C_{l_δ} for the wing equipped with the midsemispan and inboard half-span ailerons, obtained from the experimental curve of figure 11 by taking the difference between the values of C_{l_δ} at the outboard and inboard ends of each aileron, are in excellent agreement with the experimental results obtained for the wing equipped with the half-span ailerons at these two spanwise locations (table I). This excellent agreement indicates that the curve of figure 11 may be used to estimate the aileron effectiveness parameters of ailerons spanning various parts of the wing semispan on wings having plan forms similar to the wing investigated. The data indicate that an aileron of a given percent span is most effective when located outboard on the wing semispan.

The aileron effectiveness parameters for the various ailerons tested were estimated by method I of reference 10. The value of the control effectiveness parameter α_δ used in these computations was 0.54 and was obtained from section data for the NACA 64A010 airfoil equipped with an unsealed-flap-type control (reference 11), corrected for flap chord by the method of reference 10. The agreement of the experimental and empirical values is very good (fig. 11).

Yawing-moment characteristics.- For all the aileron configurations investigated, the total yawing-moment coefficient resulting from equal up and down deflection of the ailerons was approximately zero for angles of attack of less than about 8.3° and was generally adverse (sign of yawing moment opposite to sign of rolling moment) for angles of attack greater than about 8.3° (figs. 5 to 10). The ratio of adverse yawing moment to total rolling moment generally increased as the angle of attack was increased, and for some aileron configurations at high angles of attack ($\alpha \approx 20.8^{\circ}$ and 24.9°), the ratio of C_n/C_l was greater than 1. The effect of aileron span on the ratio of C_n/C_l was nonlinear. The half-span aileron located outboard on the

wing semispan had a lower ratio of adverse yaw to total rolling moment than the half-span aileron at either the midsemispan or inboard locations. The ratio of adverse yawing moment to rolling moment was considerably larger for the subject wing than the corresponding ratio obtained for the wing at 0° of sweep (reference 6). Reference 12 indicates that these large adverse yawing moments tend to reduce the rolling power of the ailerons and thereby a large rudder deflection would be required to perform a coordinated roll, especially if the airplane directional stability is low and the positive effective dihedral of the wing is large.

Aileron hinge-moment characteristics.- The variations of the hinge-moment coefficients with angle of attack and aileron deflection were nonlinear (figs. 5 to 10). The hinge-moment parameter C_{h_α} was relatively unaffected by changes in aileron span or spanwise location (fig. 11 and table I). The hinge-moment parameter C_{h_δ} was only slightly affected by changes in aileron span (fig. 11 and table I). The value of C_{h_δ} was less negative for the half-span aileron at the inboard location than at either the midsemispan or outboard locations (table I). At a given angle of attack, the rate of change of C_h with δ_a generally increased as the aileron deflection was increased except for the outboard $0.160\frac{b}{2}$ and $0.398\frac{b}{2}$ ailerons at high angles of attack where overbalance occurred for a part of the negative deflection range (figs. 5 to 10). At high angles of attack, the variation of C_h with δ_a became more nearly linear as the span of the outboard aileron was increased and as the half-span aileron was moved inboard on the wing semispan. These data for the model at 45° of sweepback show a smaller effect of aileron span on C_{h_δ} and a greater variation of C_h with δ_a at angles of attack greater than about 12° than for the model at 0° of sweep (reference 6).

A comparison of the estimated hinge-moment parameters C_{h_δ} and C_{h_α}, computed for the various spans of outboard ailerons by the method of reference 13, and the experimental values are also shown in figure 11. The estimated and experimental values of C_{h_δ} are in good agreement although the estimated data show a larger variation of C_{h_δ} with aileron span. The data show fair agreement of the values of C_{h_α} for the large-span ailerons; however, the estimated values of C_{h_α} exhibit a marked positive increase with decreasing aileron

span and there is poor agreement for the smaller-span ailerons. A study of available data indicates that the method of reference 13 generally overestimates the lifting-surface correction for small-span outboard ailerons and wings of low aspect ratios and hence the estimated values are too positive. The method is not believed to be strictly applicable to wings of aspect ratios as low as that of the subject wing. A part of the discrepancy between the estimated and experimentally determined values $\left(\text{of both } C_{h_\alpha} \text{ and } C_{h_\delta}\right)$ is attributed to the fact that the inboard end of the partial-span outboard ailerons was perpendicular to the hinge axis and not streamwise as the method of reference 13 assumes. (See fig. 1.) The centroid of the triangular area added to the aileron by this difference in end treatment is behind the centroid of the remainder of the aileron area with the result that for positive values of α the values of C_h are more negative. This differential area is a large percentage of the area of the outboard $0.160\frac{b}{2}$ aileron and, as the span of the aileron is increased, this area becomes a progressively smaller percentage of the aileron area. The effects of aileron end treatment are therefore less pronounced for the large-span ailerons.

CONCLUSIONS

A wind-tunnel investigation was made at low speed to determine the lateral control characteristics of a 45° sweptback untapered semispan wing of aspect ratio 1.59 equipped with 25-percent-chord plain unsealed ailerons having various spans and spanwise locations. The results of the investigation led to the following conclusions:

1. Existing empirical relationships for predicting the aileron effectiveness parameter C_{l_δ} and the aileron hinge-moment parameter C_{h_δ} for various spans of ailerons gave satisfactory agreement with the experimental results. The aileron hinge-moment parameter C_{h_α} could not be successfully predicted for all spans of ailerons.

2. At high angles of attack large adverse yawing moments resulted which were larger in proportion to roll for the inboard ailerons.

3. The hinge-moment parameters C_{h_α} and C_{h_δ} were only slightly affected by changes in aileron span.

Langley Aeronautical Laboratory
National Advisory Committee for Aeronautics
Langley Field, Va., December 22, 1950

REFERENCES

1. Weick, Fred E., and Jones, Robert T.: Résumé and Analysis of N.A.C.A. Lateral Control Research. NACA Rep. 605, 1937.

2. Pearson, Henry A., and Jones, Robert T.: Theoretical Stability and Control Characteristics of Wings with Various Amounts of Taper and Twist. NACA Rep. 635, 1938.

3. Langley Research Staff (Compiled by Thomas A. Toll): Summary of Lateral-Control Research. NACA Rep. 868, 1947.

4. Johnson, Harold S., and Hagerman, John R.: Wind-Tunnel Investigation at Low Speed of a 45° Sweptback, Untapered Semispan Wing of Aspect Ratio 1.59 Equipped with Various 25-Percent-Chord Plain Flaps. NACA TN 2169, 1950.

5. Johnson, Harold S., and Hagerman, John R.: Wind-Tunnel Investigation at Low Speed of an Unswept Untapered Semispan Wing of Aspect Ratio 3.13 Equipped with Various 25-Percent-Chord Plain Flaps. NACA TN 2080, 1950.

6. Johnson, Harold S., and Hagerman, John R.: Wind-Tunnel Investigation at Low Speed of the Lateral Control Characteristics of an Unswept Untapered Semispan Wing of Aspect Ratio 3.13 Equipped with Various 25-Percent-Chord Plain Ailerons. NACA TN 2199, 1950.

7. Polhamus, Edward C.: Jet-Boundary-Induced-Upwash Velocities for Swept Reflection-Plane Models Mounted Vertically in 7- by 10-Foot, Closed, Rectangular Wind Tunnels. NACA TN 1752, 1948.

8. Herriot, John G.: Blockage Corrections for Three-Dimensional-Flow Closed-Throat Wind Tunnels, with Consideration of the Effect of Compressibility. NACA RM A7B28, 1947.

9. Swanson, Robert S., and Toll, Thomas A.: Jet-Boundary Corrections for Reflection-Plane Models in Rectangular Wind Tunnels. NACA Rep. 770, 1943.

10. Lowry, John G., and Schneiter, Leslie E.: Estimation of Effectiveness of Flap-Type Controls on Sweptback Wings. NACA TN 1674, 1948.

11. Dods, Jules B., Jr.: Wind-Tunnel Investigation of Horizontal Tails. IV- Unswept Plan Form of Aspect Ratio 2 and a Two-Dimensional Model. NACA RM A8J21, 1948.

12. Fehlner, Leo F.: A Study of the Effect of Adverse Yawing Moment on Lateral Maneuverability at a High Lift Coefficient. NACA ARR, Sept. 1942.

13. Toll, Thomas A., and Schneiter, Leslie E.: Approximate Relations for Hinge-Moment Parameters of Control Surfaces on Swept Wings at Low Mach Numbers. NACA TN 1711, 1948.

TABLE I

DIMENSIONAL CHARACTERISTICS AND LATERAL-CONTROL PARAMETERS OF VARIOUS 0.25c AILERONS

TESTED ON 45° SWEPTBACK SEMISPAN WING OF ASPECT RATIO 1.59

Configuration	Aileron span, $\frac{b_a}{b/2}$	Aileron spanwise location		M_1 (ft^3)	C_{l_δ}	C_{h_δ}	C_{h_α}
		$\frac{y_{a_i}}{b/2}$	$\frac{y_{a_o}}{b/2}$				
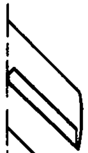	0.875	0.080	0.955	0.7216	0.00111	-0.0037	-0.0011
	.637	.318	.955	.5686	.00102	-.0044	-.0012
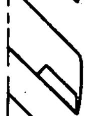	.398	.557	.955	.3855	.00077	-.0044	-.0011
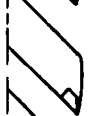	.160	.795	.955	.2024	.00040	-.0035	-.0015
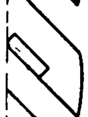	.477	.080	.557	.3361	.00036	-.0030	-.0010
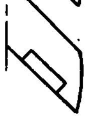	.477	.318	.795	.3662	.00063	-.0045	-.0007

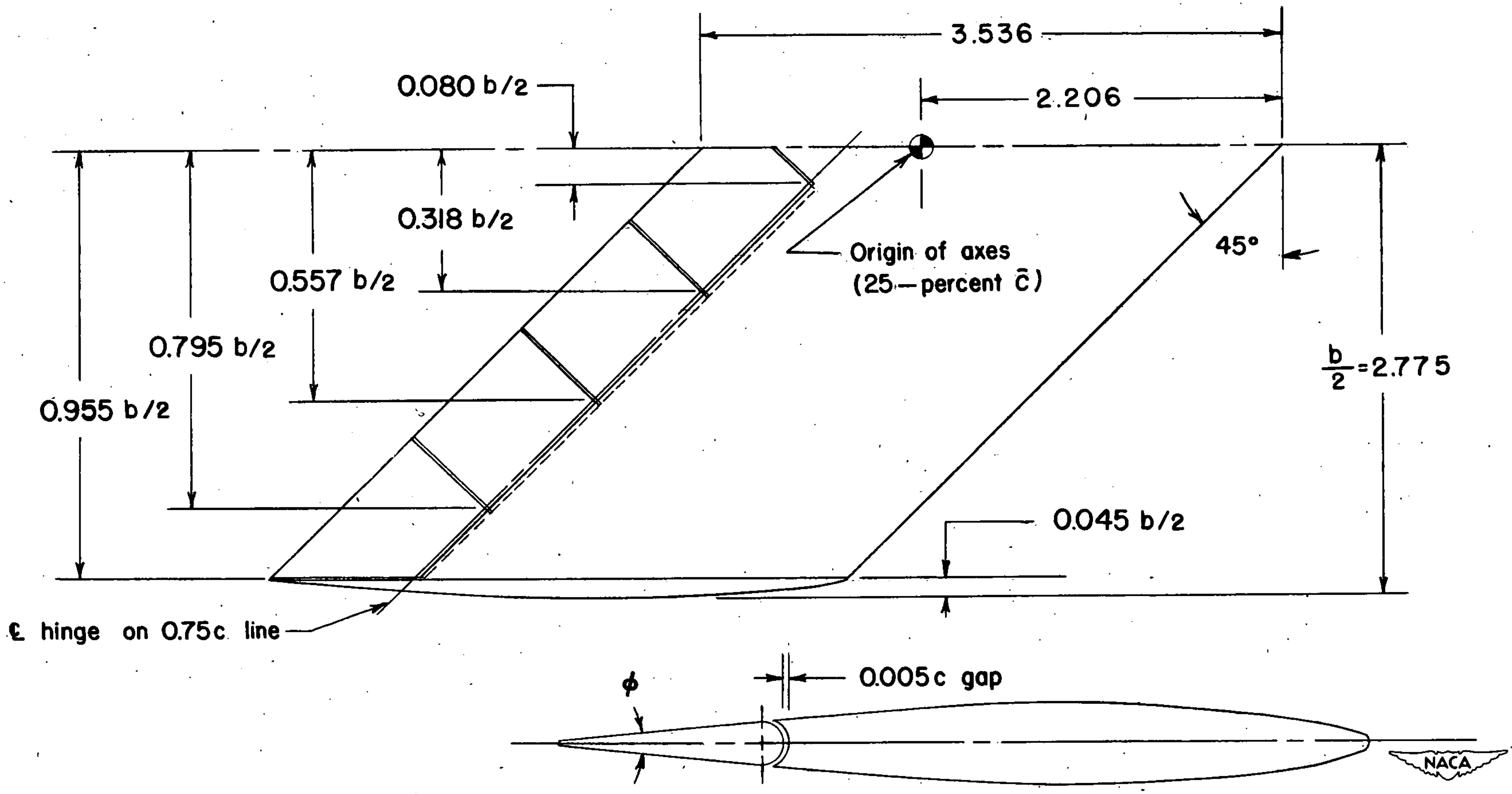

Figure 1.- Drawing of the 45° sweptback-semispan-wing model having an aspect ratio of 1.59. NACA 64A010 airfoil section normal to leading edge. Trailing-edge angle ϕ measured perpendicular to hinge axis is 12.0° and measured parallel to free stream is 8.5°. (All dimensions are in ft.)

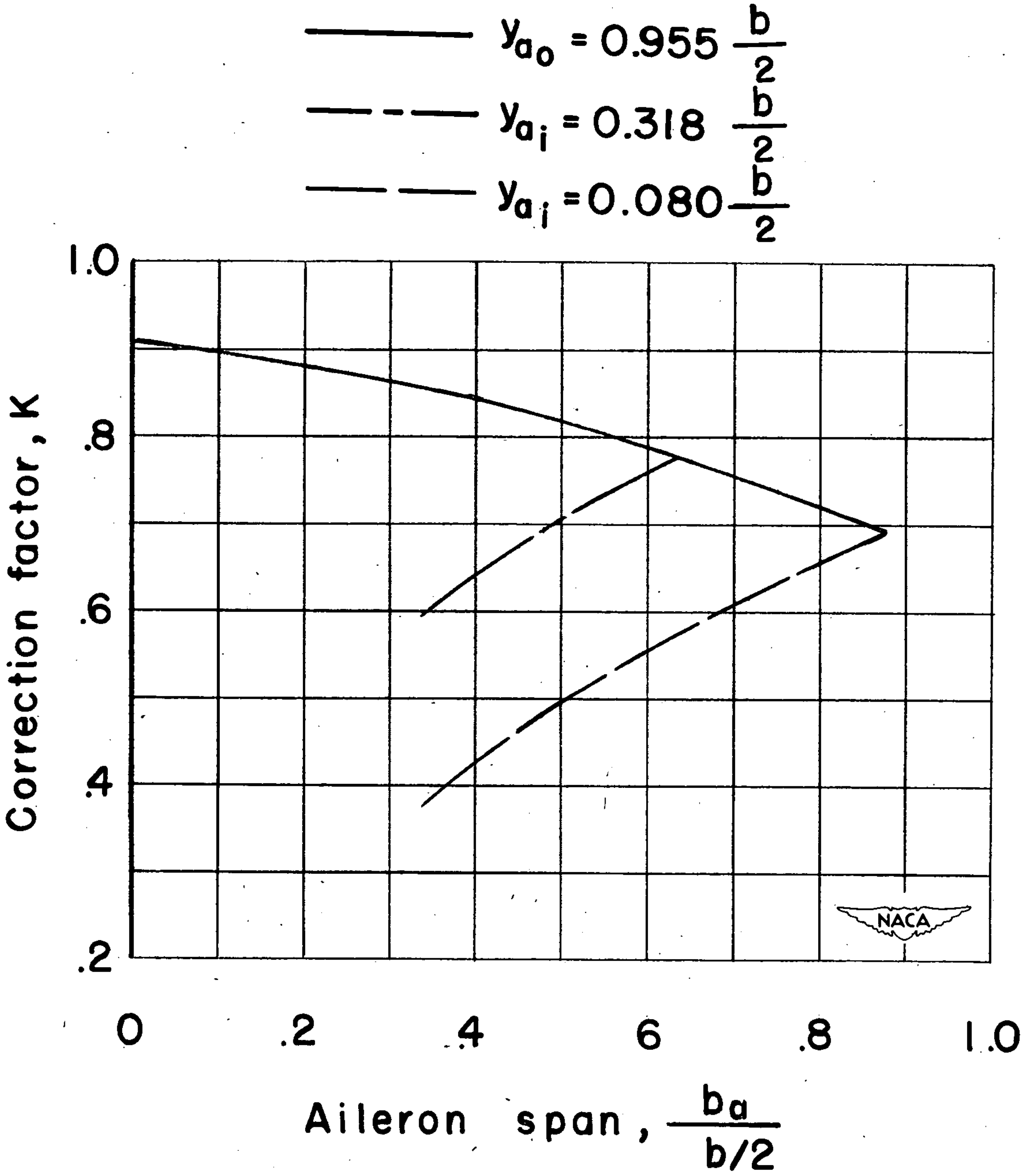

Figure 2.- Reflection-plane correction factor for rolling-moment coefficients $\left(C_l = KC_{l_{measured}}\right)$.

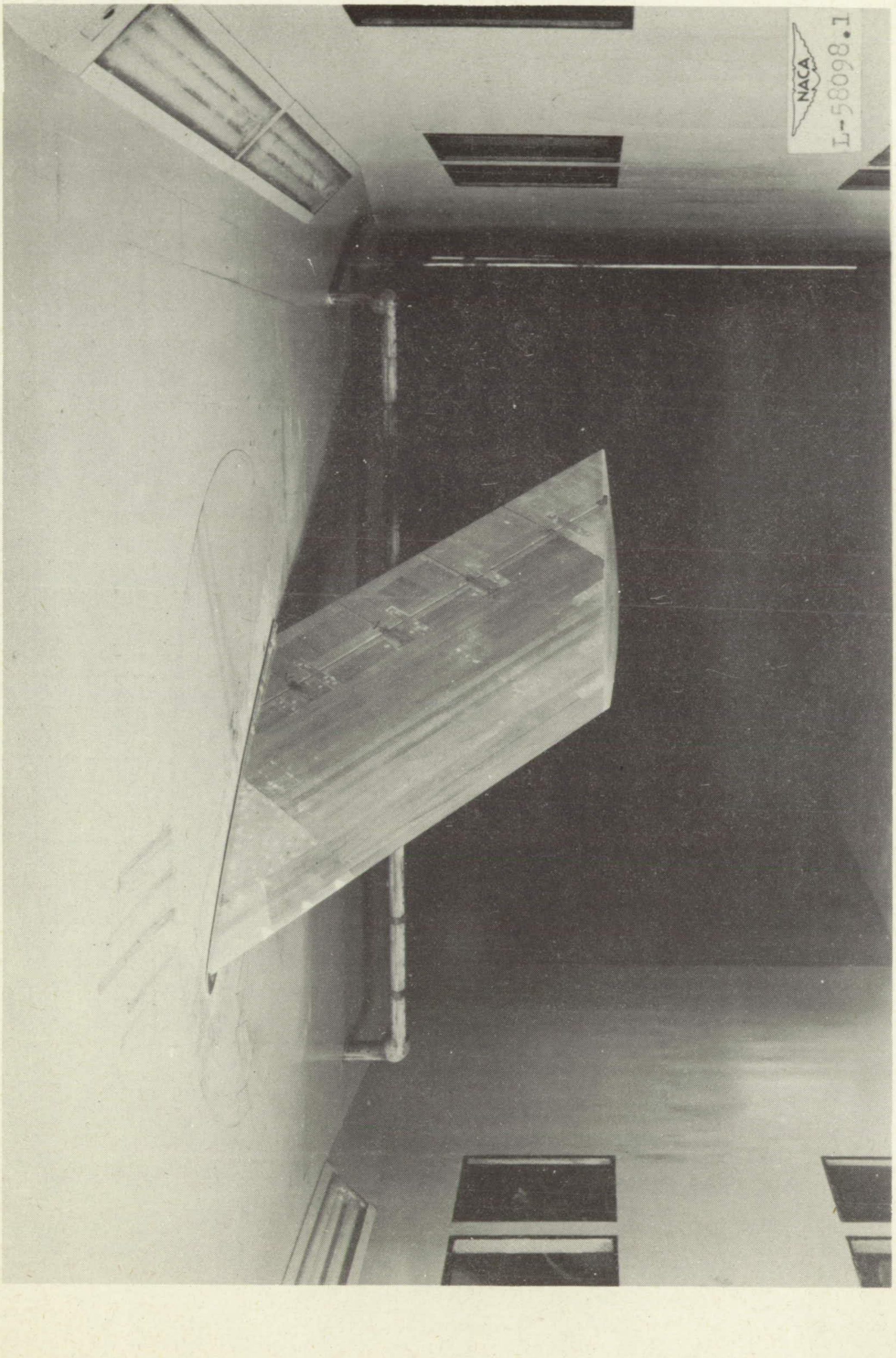

Figure 3.- The 45° sweptback-semispan-wing model having an aspect ratio of 1.59 mounted in the Langley 300 MPH 7- by 10-foot tunnel.

Page intentionally left blank

Page intentionally left blank

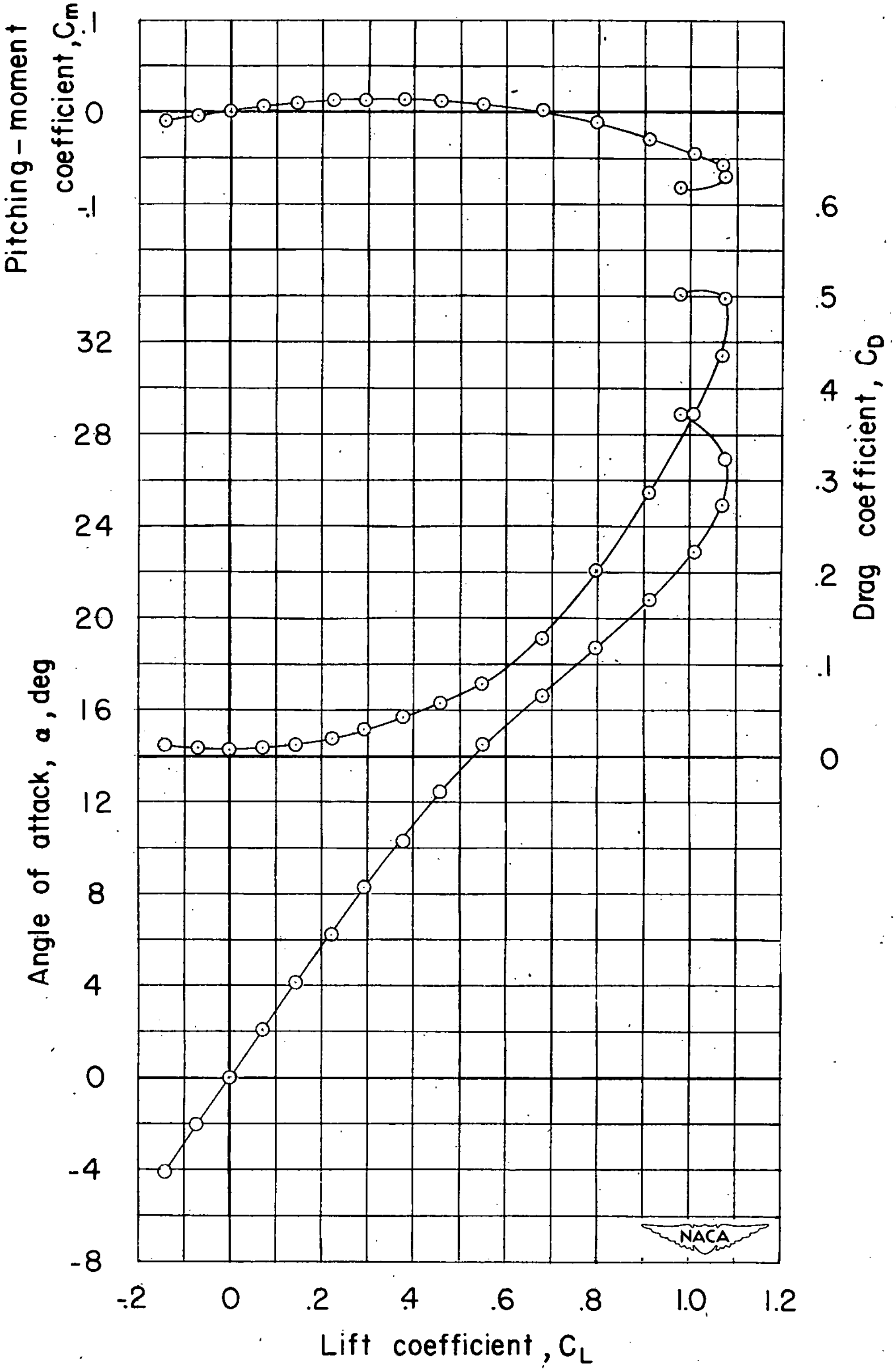

Figure 4.- Aerodynamic characteristics in pitch of the plain 45° sweptback semispan wing having an aspect ratio of 1.59.

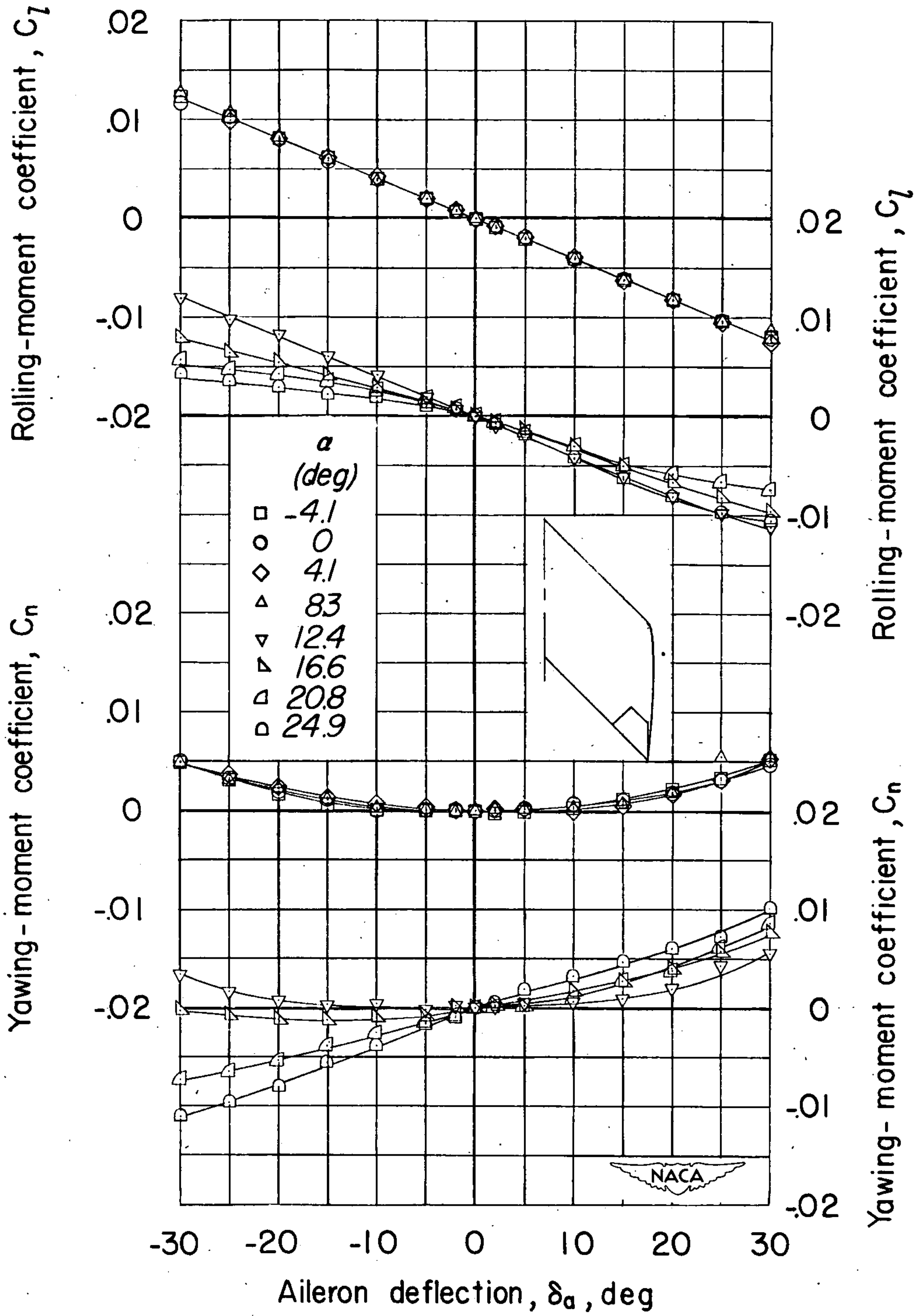

Figure 5.- Variation of lateral control characteristics with aileron deflection on the 45° sweptback semispan wing having an aspect ratio of 1.59. $b_a = 0.160\frac{b}{2}$; $y_{a_i} = 0.795\frac{b}{2}$; $y_{a_o} = 0.955\frac{b}{2}$.

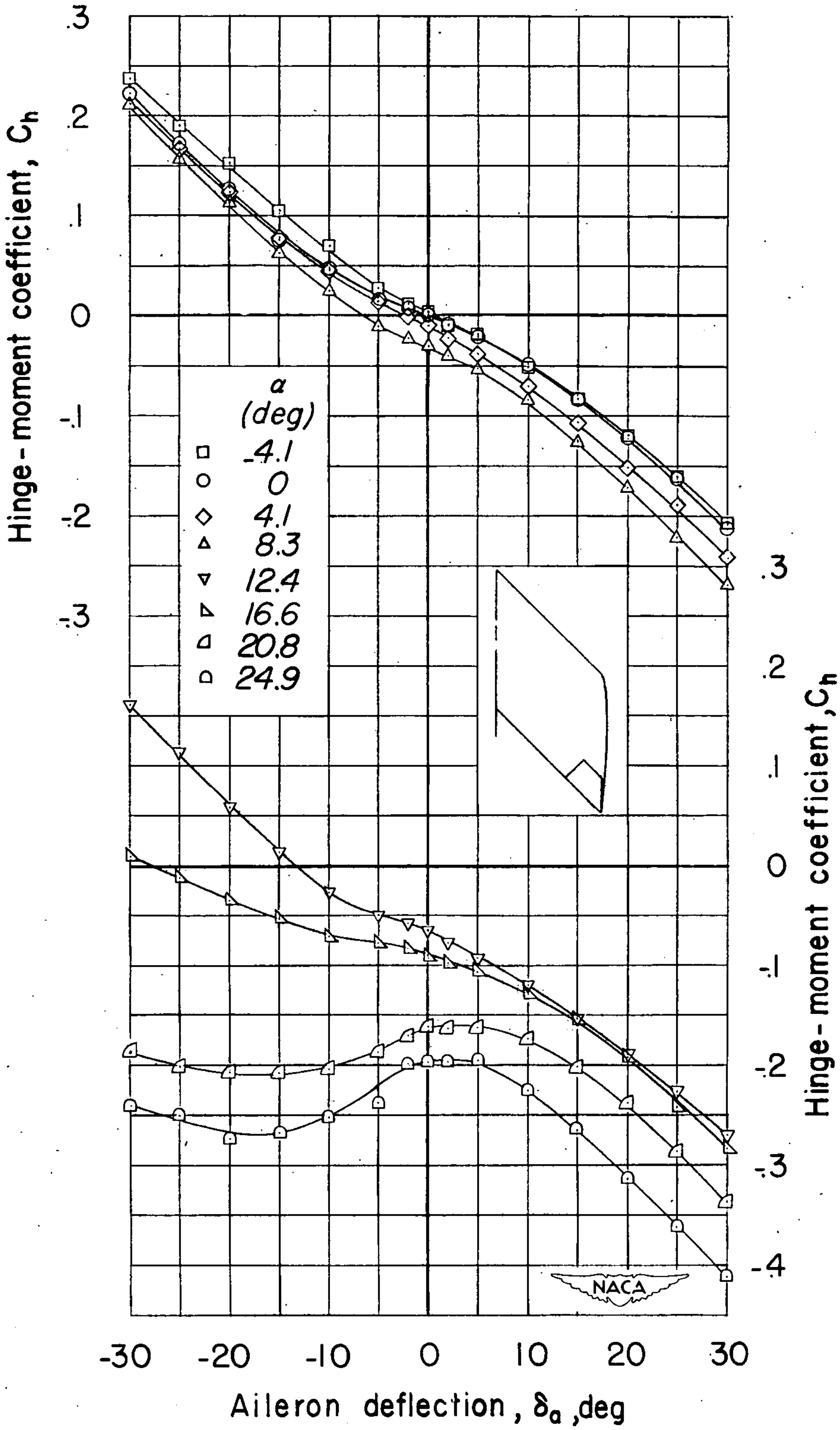

Figure 5.- Concluded.

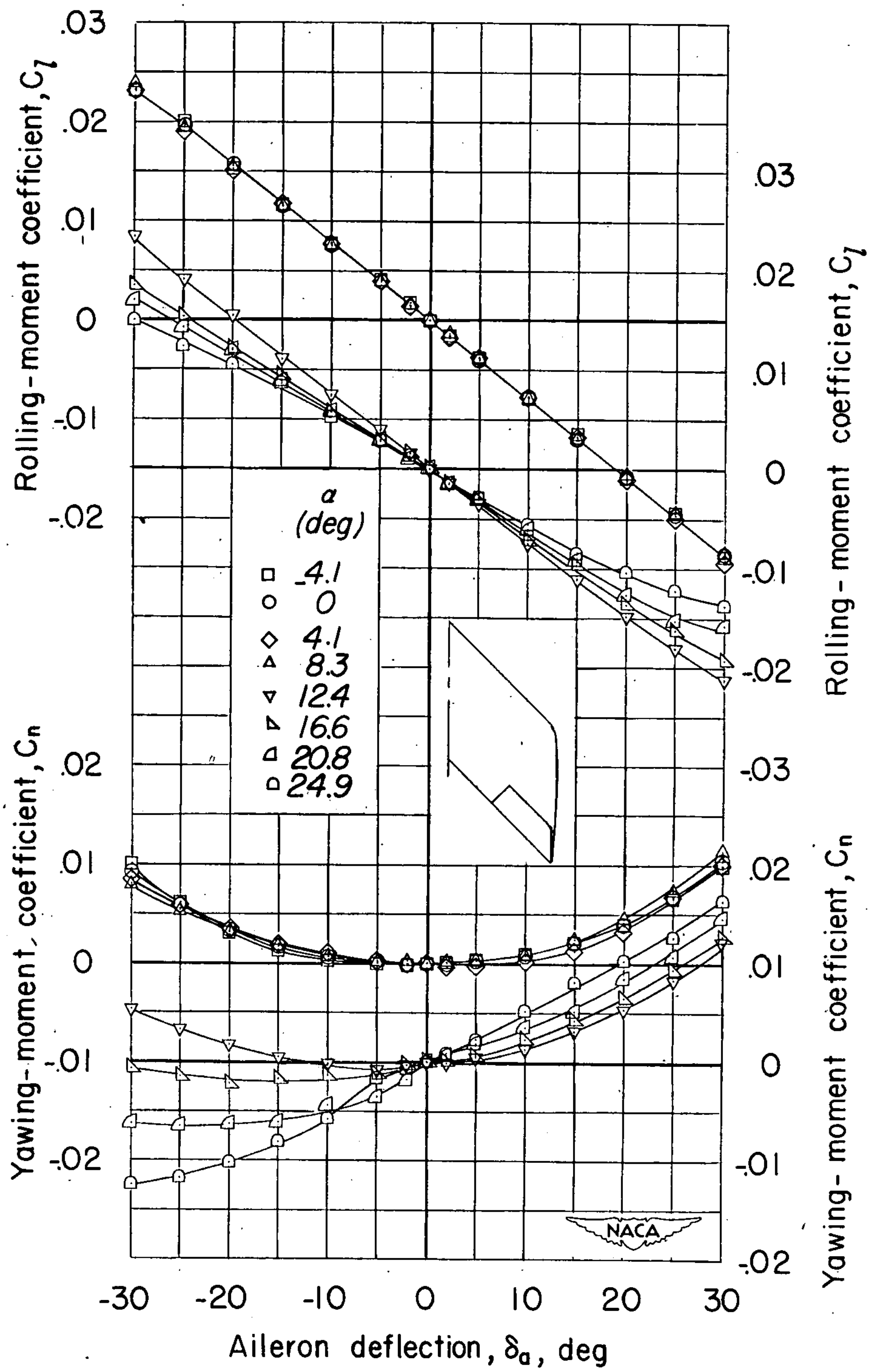

Figure 6.- Variation of lateral control characteristics with aileron deflection on the 45° sweptback semispan wing having an aspect ratio of 1.59. $b_a = 0.398\frac{b}{2}$; $y_{a_i} = 0.557\frac{b}{2}$; $y_{a_o} = 0.955\frac{b}{2}$.

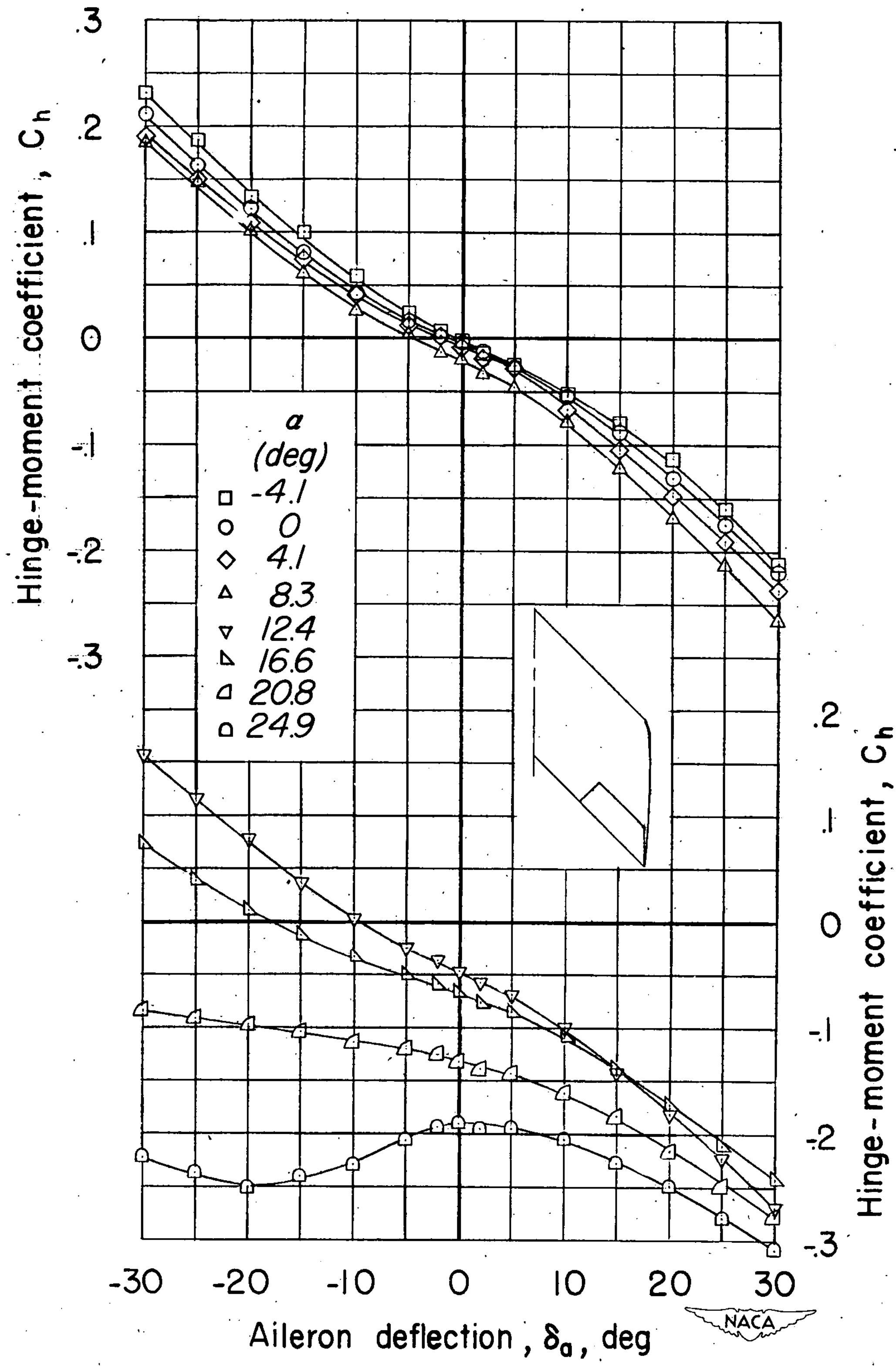

Figure 6.- Concluded.

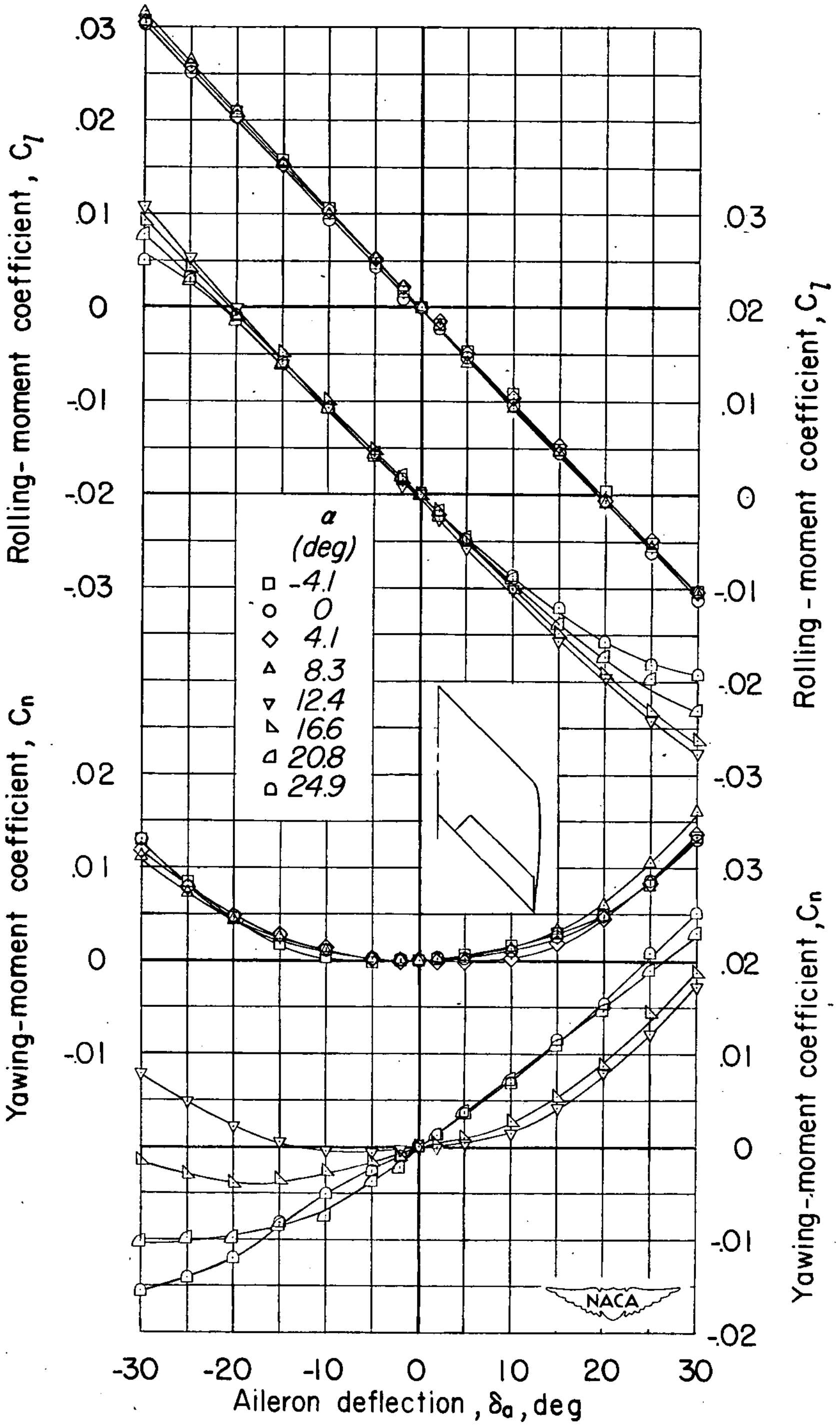

Figure 7.- Variation of lateral control characteristics with aileron deflection on the 45° sweptback semispan wing having an aspect ratio of 1.59. $b_a = 0.637\frac{b}{2}$; $y_{a_i} = 0.318\frac{b}{2}$; $y_{a_o} = 0.955\frac{b}{2}$.

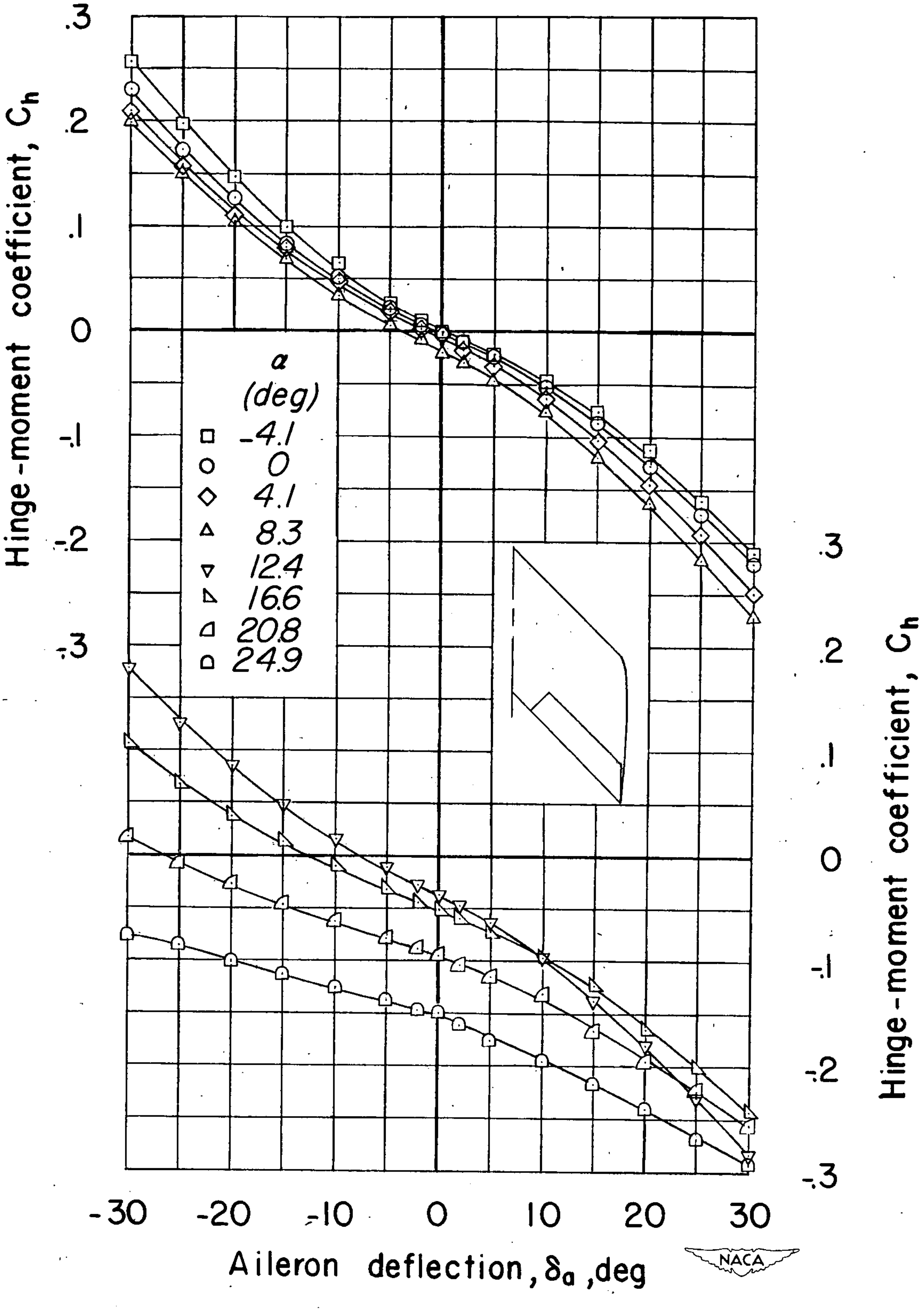

Figure 7.- Concluded.

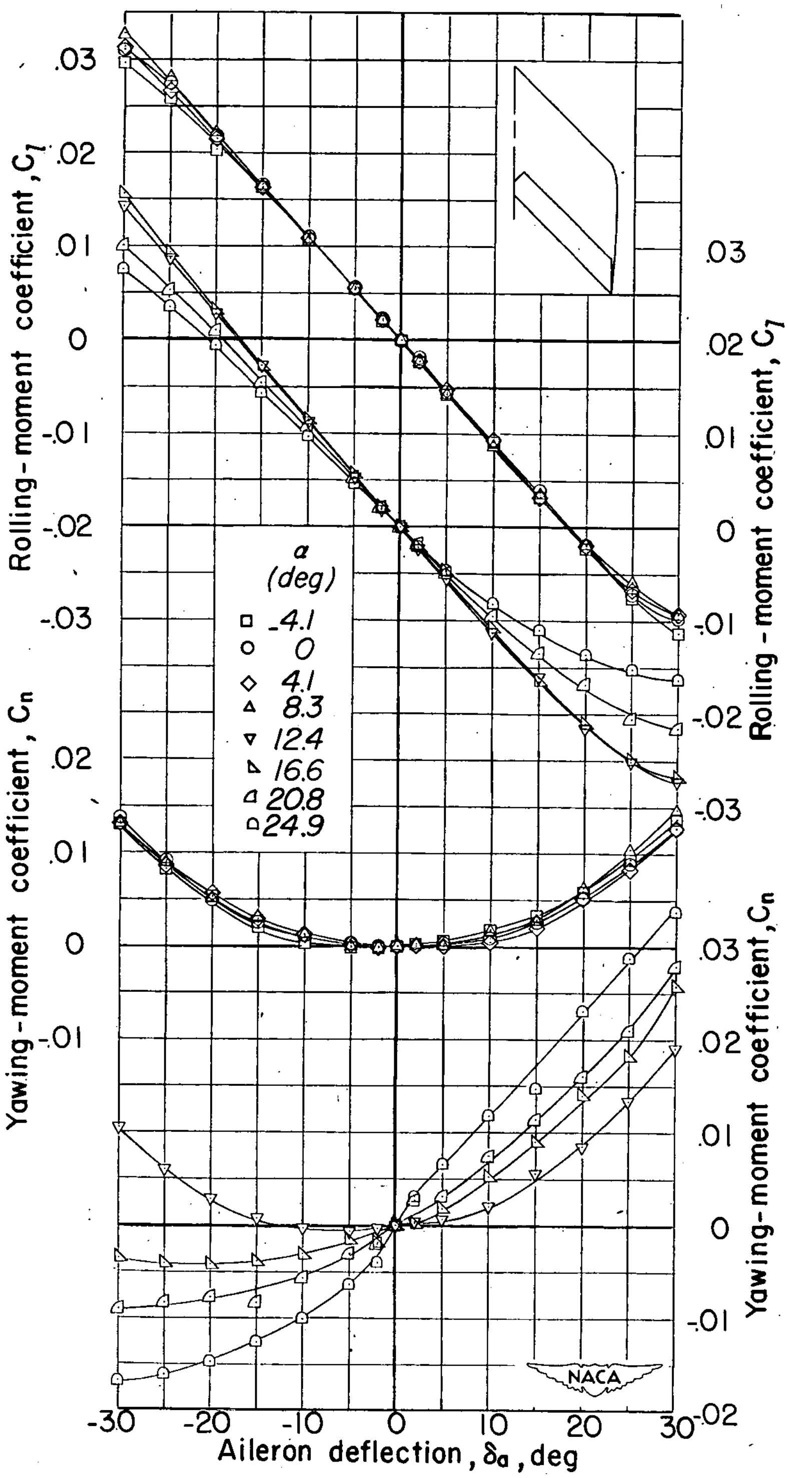

Figure 8.- Variation of lateral control characteristics with aileron deflection on the 45° sweptback semispan wing having an aspect ratio of 1.59. $b_a = 0.875\frac{b}{2}$; $y_{a_i} = 0.080\frac{b}{2}$; $y_{a_o} = 0.955\frac{b}{2}$.

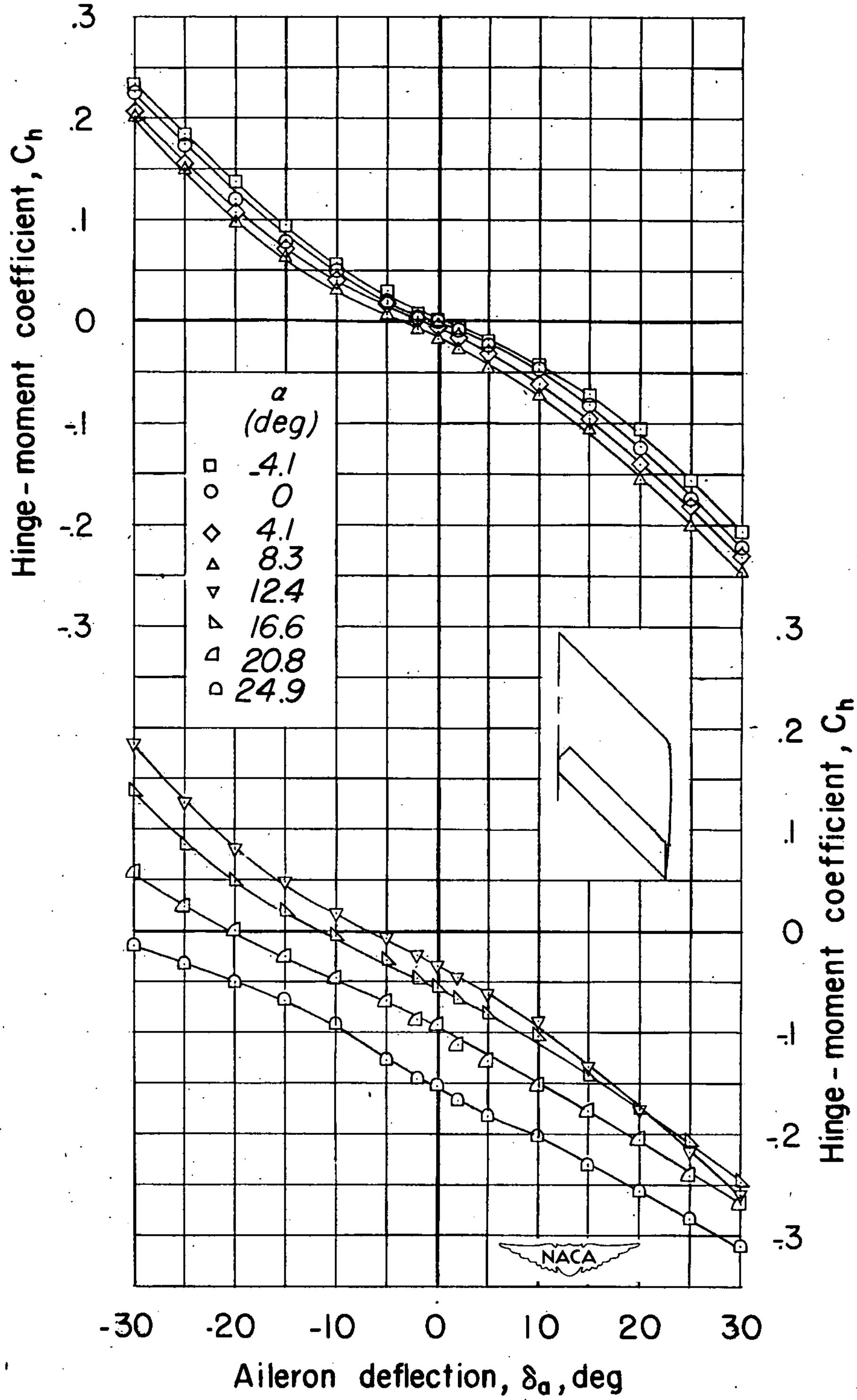

Figure 8.- Concluded.

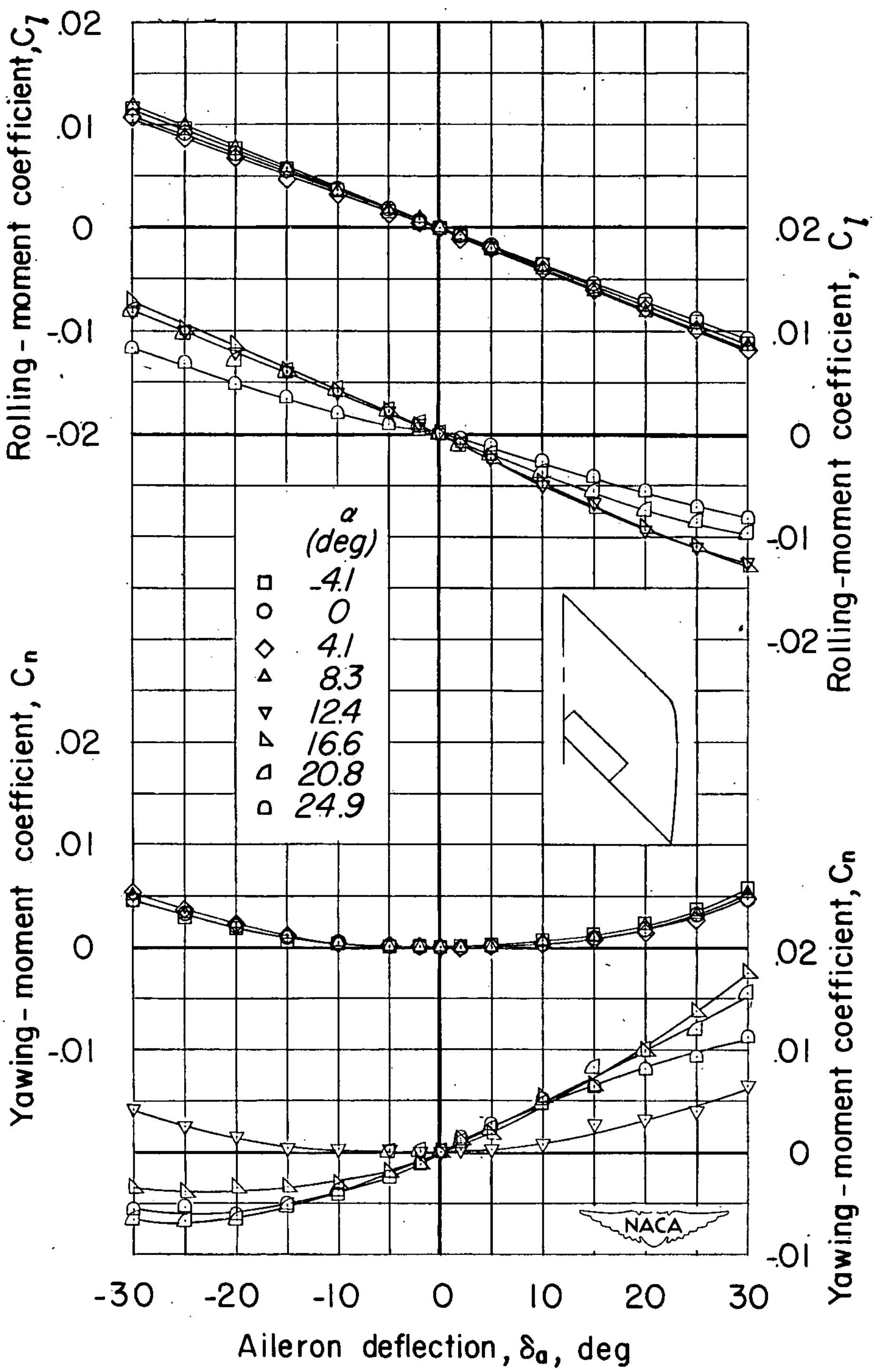

Figure 9.- Variation of lateral control characteristics with aileron deflection on the 45° sweptback semispan wing having an aspect ratio of 1.59. $b_a = 0.477\frac{b}{2}$; $y_{a_i} = 0.080\frac{b}{2}$; $y_{a_o} = 0.557\frac{b}{2}$.

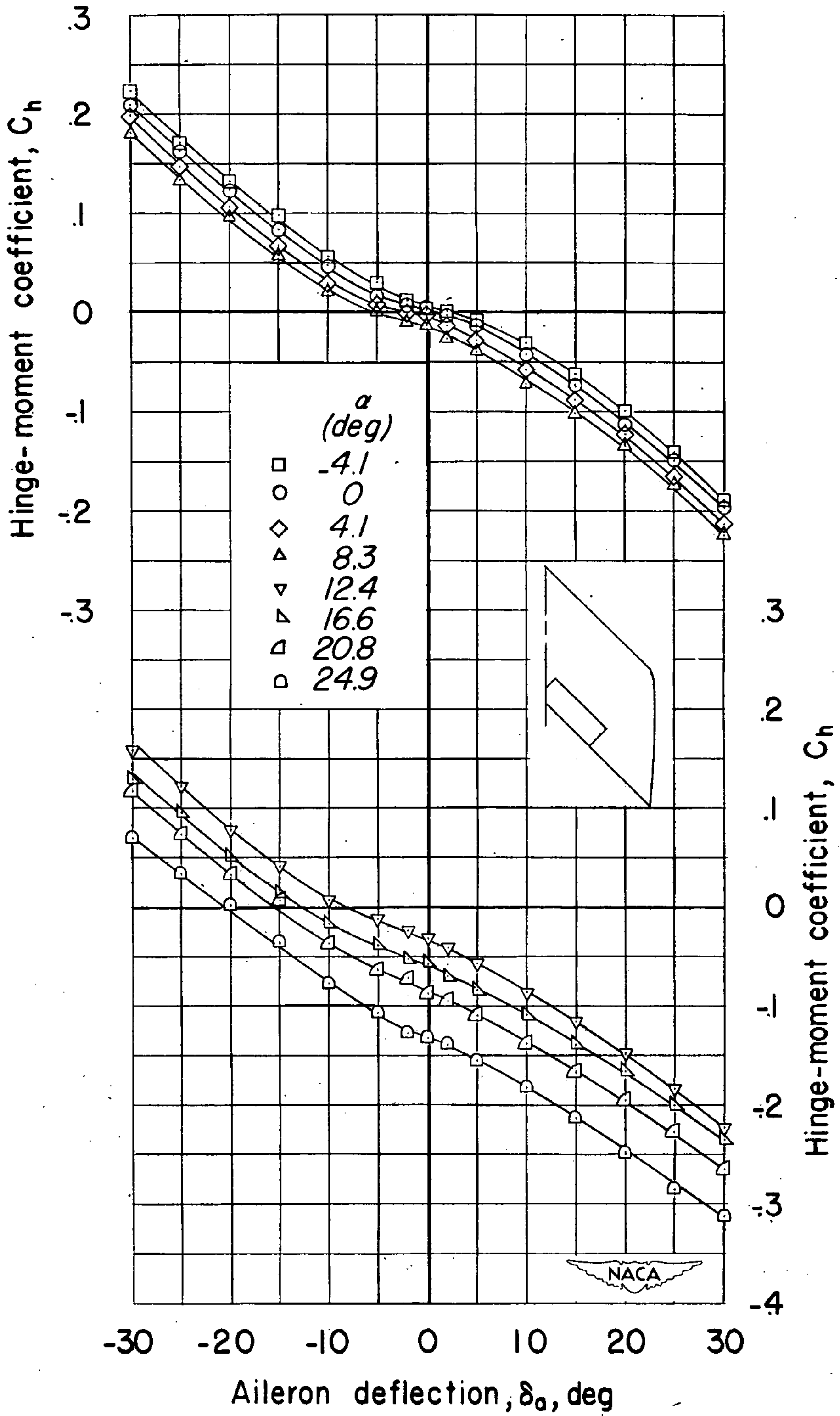

Figure 9.- Concluded.

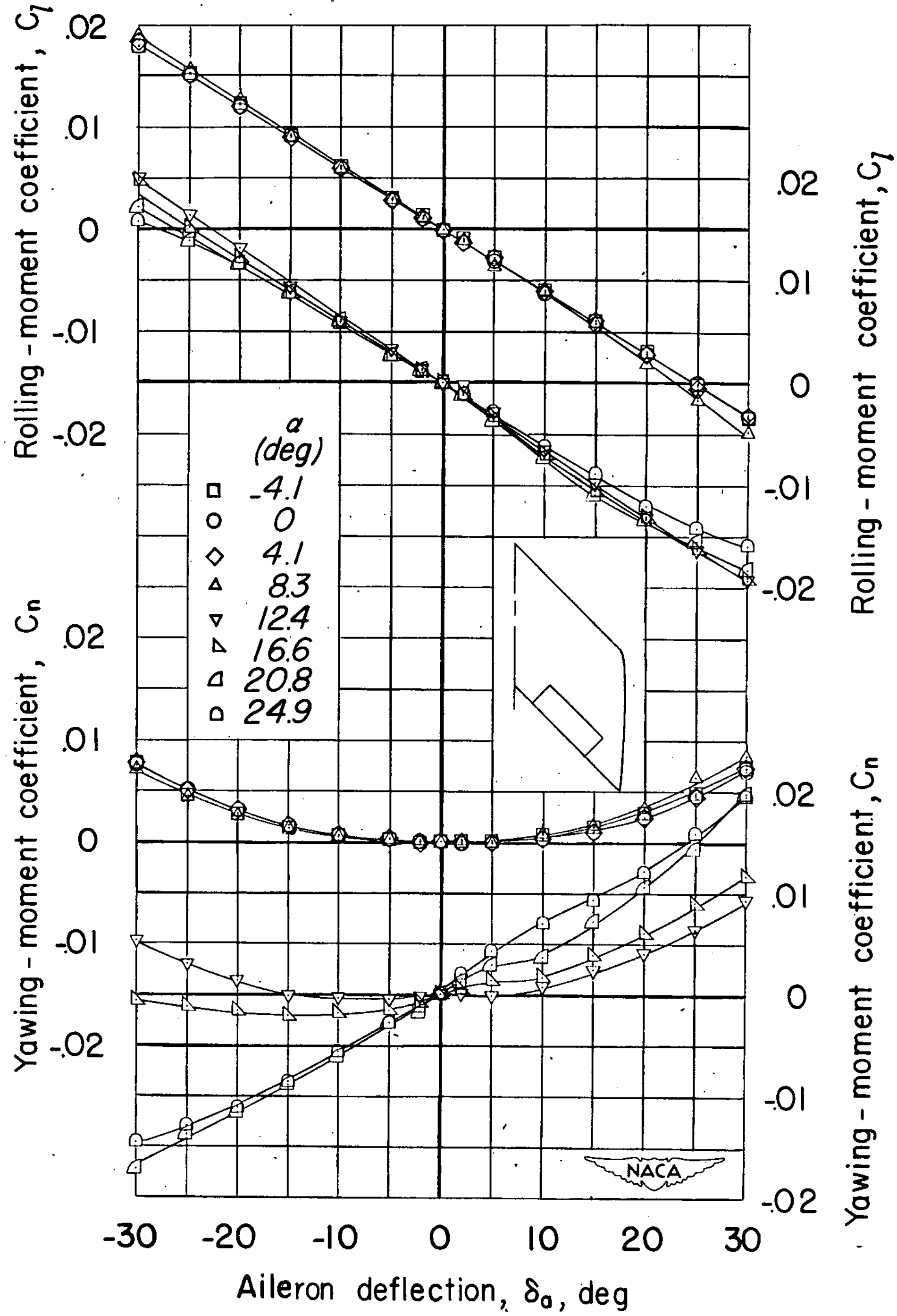

Figure 10.- Variation of lateral control characteristics with aileron deflection on the 45° sweptback semispan wing having an aspect ratio of 1.59. $b_a = 0.477\frac{b}{2}$; $y_{a_i} = 0.318\frac{b}{2}$; $y_{a_o} = 0.795\frac{b}{2}$.

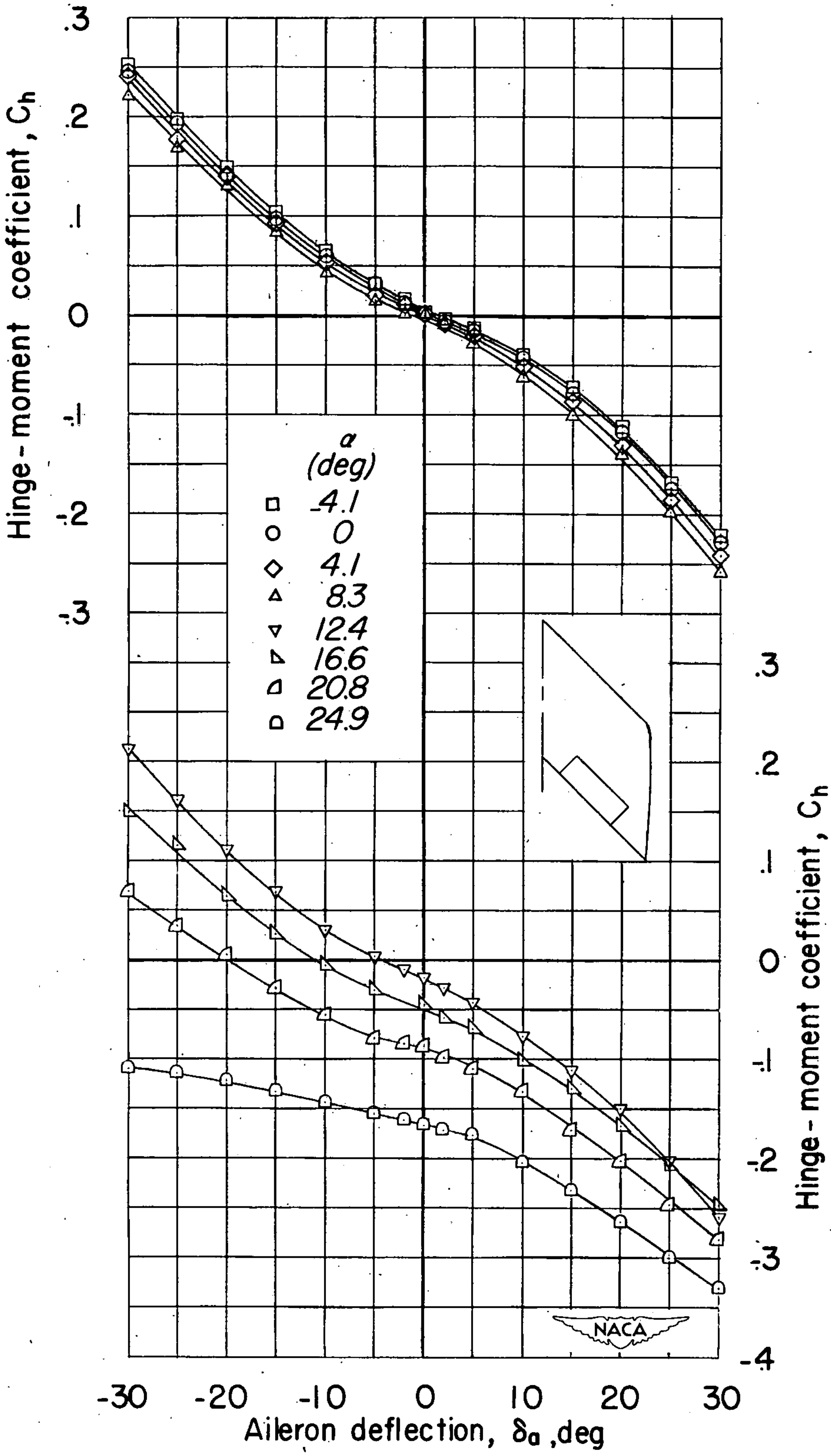

Figure 10.- Concluded.

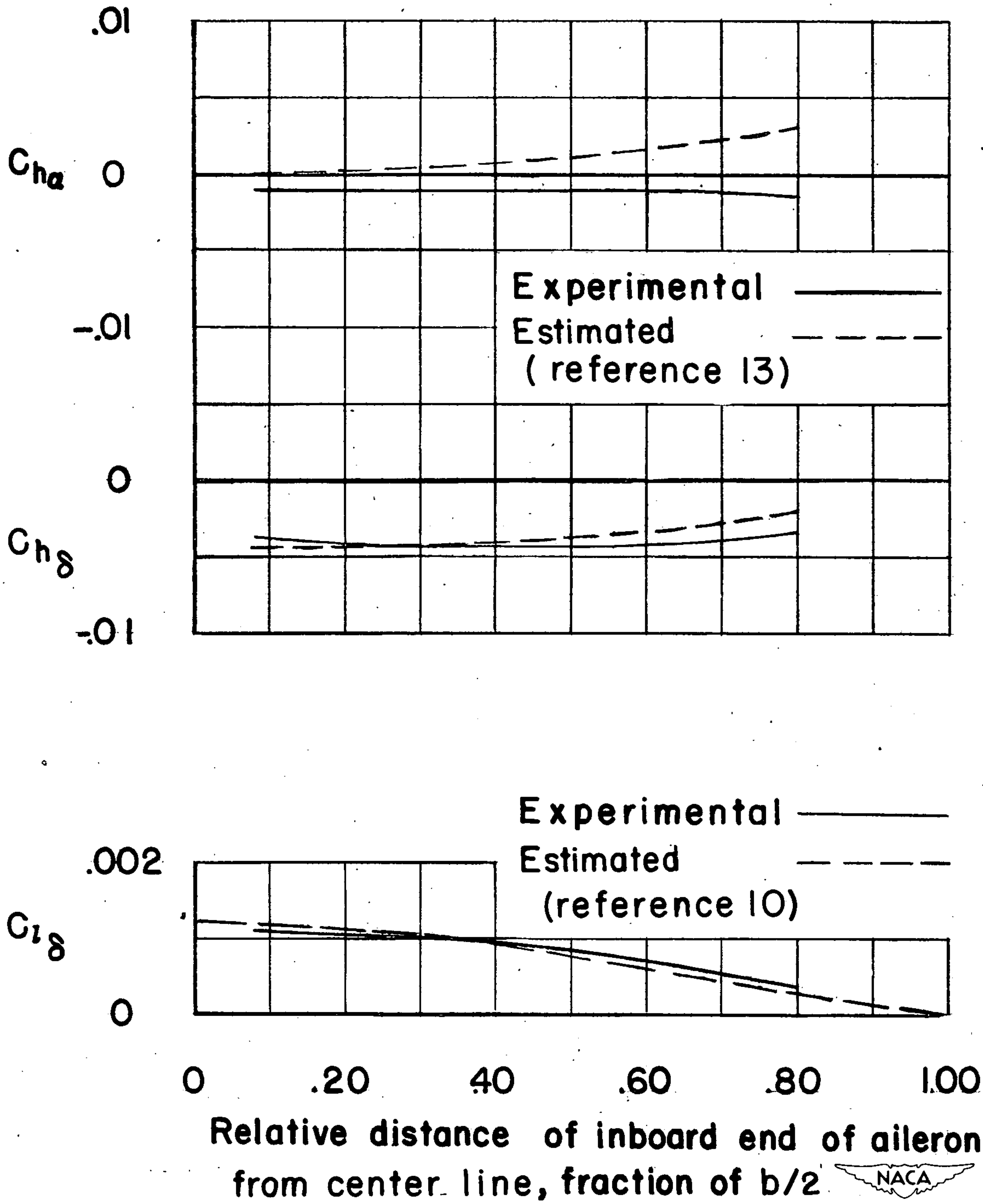

Figure 11.- Variation of aileron parameters C_{h_α}, C_{h_δ}, and C_{l_δ} with relative position of inboard end of aileron on the 45° sweptback semispan wing having an aspect ratio of 1.59. $y_{a_o} = 0.955\frac{b}{2}$.